Muscle hypertrophy and neuroplasticity in the small bowel in Short Bowel Syndrome

Rasul Khasanov (Rasul.Khasanov@medma.uni-heidelberg.de)
University Hospital Mannheim, Medical Faculty Mannheim of Heidelberg University
Daniel Svoboda
University Hospital Mannheim, Medical Faculty Mannheim of Heidelberg University
María Ángeles Tapia-Laliena
University Hospital Mannheim, Medical Faculty Mannheim of Heidelberg University
Martina Kohl
University Medical Center Schleswig-Holstein
Silke Maas-Omlor
Enteric Nervous system Group University of Applied Sciences Kaiserslautern
Cornelia Irene Hagl
Carl Remigius Medical School
Lucas M. Wessel
University Hospital Mannheim, Medical Faculty Mannheim of Heidelberg University
Karl-Herbert Schäfer
Enteric Nervous system Group University of Applied Sciences Kaiserslautern

Research Article

Keywords: Enteric Neurons, ENS, Nestin, PGP 9.5, Short Bowel Syndrome, Bowel resection

Posted Date: October 6th, 2022

DOI: https://doi.org/10.21203/rs.3.rs-2117961/v1

Additional Declarations: No competing interests reported.

Version of Record: A version of this preprint was published at Histochemistry and Cell Biology on July 3rd, 2023. See the published version at https://doi.org/10.1007/s00418-023-02214-4.

Abstract

Short bowel syndrome (SBS) is a severe, life-threatening condition and one of the leading causes of intestinal failure in children. Here we were interested in changes in muscle layers and especially in the myenteric plexus of the enteric nervous system (ENS) of the small bowel in the context of intestinal adaptation.

Twelve rats underwent a massive resection of the small intestine to induce an SBS. Sham laparotomy without small bowel transection was performed in 10 rats. Two weeks after surgery, the remaining jejunum and ileum were harvested and studied. Samples of human small bowel were obtained from patients who underwent resection of small bowel segments due to a medical indication. Morphological changes in the muscle layers and the expression of nestin, a marker for neuronal plasticity, were studied.

Following a SBS, muscle tissue increases significantly in both parts of the small bowel, jejunum, and ileum. The leading pathophysiological mechanism of these changes is hypertrophy. Additionally, we observed an increased nestin expression in the myenteric plexus in the remaining bowel of SBS.

Our human data also showed that in patients with SBS, the proportion of stem cells in the myenteric plexus have risen by more than two times.

Our findings suggest that the ENS is tightly connected with changes in intestinal muscle layers and is critically involved in the intestinal adaptation process to SBS.

Introduction

Short bowel syndrome (SBS) is a severe, life-threatening condition and one of the leading causes of intestinal failure in children, due to massive bowel resection or loss of resorptive area, the absorption of the remaining intestine is not sufficient, causing maldigestion and malabsorption (Goulet and Sauvat 2006; Oliveira et al. 2012).

Accordingly, intestinal adaptation after extensive small bowel resection is crucial for enhancing the absorptive and digestive capacity. The functional and structural changes in intestinal adaptation comprises smooth muscle hyperplasia, enterocyte proliferation (O'Brien et al. 2001; Oliveira et al. 2012; Martin et al. 2008), increased villus height, crypt depth, and changes in binding proteins and receptors (Stephens et al. 2010; Stern et al. 2000; Vomhof-DeKrey et al. 2021; Sukhotnik et al. 2016). However, to date, most of the studies on the SBS adaptation were mainly focused on intestinal epithelium and the role of growth and angiogenetic factors (McMellen et al. 2010; Tappenden 2014a; Lin et al. 2019; Martin et al. 2009).

Usually many patients with SBS suffer from relevant pathological dilatation of the remaining small intestine, including the formation of reservoirs and stasis of intestinal contents. Clinically, these changes are manifested by increased malabsorption and maldigestion, excessive proliferation of bacterial microflora in the small intestine, which leads to complications such as bacterial overgrowth, D-lactate acidosis, translocation of intestinal bacteria into extraintestinal organs and, mucosal ulceration with the development of intestinal bleeding (Weih et al. 2012; Ives et al. 2016).

The basis for dilatation of the small intestine could be induced by changes in the muscle layers of the small intestine or alterations within the intrinsic nervous system of the gut, the enteric nervous system (ENS). Although there is no literature consensus about the role of the muscle layers in the small intestine adaptation after SBS (Chen et al. 2012; Chen et al. 2015; Chen et al. 2013; Martin et al. 2008), some studies have already described that reduced

ENS function enhances intestinal mucosal adaptation after massive small bowel resection (Garcia et al. 1999; Hitch et al. 2012). Also, the ENS participates in the GLP-2 peptide pathway, which is known to enhance intestinal adaptation and regulates several intestinal adaptive processes, including epithelial proliferation, apoptosis, and inflammation (Kaunitz and Akiba 2019; Fleming et al. 2020). Moreover the ENS adapts itself continuously to environmental changing conditions like diet (Fichter et al. 2011), mechanical bowel movements, inflammatory responses (Collins et al. 1992) and the microbiome (Grundmann et al. 2016), which strongly influence neuronal differentiation and plasticity. The ENS also regulates primary gut functions such as peristalsis, electrolyte secretion, and blood supply (Furness 2012). Furthermore, the ENS interacts with the intrinsic gut immune system (Wood 2004; Niesler et al. 2021).

Importantly, the ENS is crucial for bowel motility. For instance, in conditions like Hirschsprung`s disease, where parts of ENS are absent or reduced, the affected part of the gut has no peristaltic or propulsive motility (Lotfollahzadeh et al. 2021). Here, the neuronal homeostasis seems to be maintained by new neurons formed from myenteric ganglia precursor cells. These neuronal precursors express both nestin and p75NTR, but not the pan-glial marker Sox10 (Kulkarni et al. 2017). Therefore, nestin acts as neuronal precursor marker (Grundmann et al. 2016).

However, the direct influence of ENS on intestinal adaptation after massive small bowel resection has not been described yet.

Since it is known that both the ENS and intestinal smooth muscles are tightly connected, we designed this study to analyse the role of both smooth muscle tissue and the ENS on the intestinal adaptation after massive small bowel resection on animal models.

Our findings suggest that ENS is tightly connected with changes in intestinal muscle layers and is critically involved in the intestinal adaptation process to SBS.

Material And Methods

Animals and Tissue collection

Animal experiments were conducted with the approval of the local ethic committee (Luebeck University, V 312-72241.122-24 (43 – 3/06)) on adult Wistar rats (260–360 g). Twelve rats underwent a massive resection of the small intestine to induce an SBS (rSBS) as described before (Lei et al. 2011). Rats were anesthetized with an intraperitoneal injection of Ketamine (40 mg/kg) and Rompun (4 mg/kg). The small intestine was resected, leaving 10 cm jejunum and 5 cm ileum, so approximately 80% of the small intestine was resected. Finally, a marking suture was applied 5 cm oral to the anastomosis. After bowel resection in the rSBS group, end-to-end anastomoses with interrupted Vicryl 6/0 sutures were performed. Simultaneously, a sham laparotomy without small bowel transection was performed in 10 rats, and these animals were used as controls. In the control group, marking sutures on the small bowel 10 and 5 cm adjacent to the colon were applied. One rat out of twelve in rSBS group died during the surgery. No antibiotics were administered. In general, rats with SBS lost 10–15% of their original body weight during the first week. By the end of the second week, most animals had regained their preoperative weight.

Two weeks after surgery, all animals were killed by cervical dislocation, and the remaining jejunum and ileum were harvested. The lumen was flushed with ice-cold phosphate-buffered saline before further processing. The specimens orally and anally from intestinal anastomosis were harvested and marked as jejunum and ileum samples, correspondingly. The samples were fixed in 4% formaldehyde overnight, embedded in paraffin, sectioned

at 5 µm thickness, and processed for hematoxylin-eosin (HE), Picrosirius red and immunohistochemical stainings (smoth muscle actin and nestin).

Immunohistochemical staining

HE staining was conducted according to the standard protocol with the Leica autostainer LX.

Serial paraffin-embedded sections of small bowel were stained with Picrosirius Red according to the manufacturer's protocol, using a commercial kit (Nr. 13425 Morphisto, Frankfurt am Main, Germany). Briefly, paraffin-embedded sections were deparaffinized and rehydrated through a series of xylene and graded alcohol washes, followed by staining with Weigert iron-hematoxylin for 15 min. Slides were rinsed in distilled water, washed for 8 min. in running tap water and again rinsed in distilled water. Afterwards slides were stained for 1 h in a Sirius Red solution. Next, the sections were treated with Acetic acid 30% twice for 1 min. Slides were submersed in 96% ethanol twice for 4 min., quickly dehydrated in graded ethyl alcohols, cleared with xylene, and mounted with xylene-based mounting medium (Nr. 13425 Morphisto, Frankfurt am Main, Germany).

Smooth muscle actin staining was started with standard deparaffinization and rehydration (70%, 80%, 90%, 2× 100% ethanol, 3× Xylol; 30 s each) of the slides. Unmasking the antigens was performed in a steamer in Tris-EDTA-Buffer pH9,0 (DAKO K8002); permeabilization was for 10 min. with 0.5% Triton X100; blocking with Normal Goat Serum (1:10; DAKO X0907) for 30 min. The incubation of mouse-anti-smooth muscle actin AF 594nm (1:100; Santa Cruz: sc-53142) was for 1 hour. Finally, samples were incubated with DAPI and mounted.

Regarding, Nestin peroxidase staining, it was performed with the ENVISION KIT (DAKO) as follows: unmasking with citrate buffer pH 6.0 (DAKO S2369) at 95ºC for 1h; blocking with 5% BSA (Serva 11930) for 1h. Incubation with mouse-anti-nestin (1:200; Chemicon Int) for 1h. After incubation with 3% hydrogen peroxide, samples were incubated with DAKO EnVision + System-HRP labelled polymer anti-Mouse (DAKO K4000) as a secondary antibody and visualized with DAB Substrat-Chromogen Set (DAKO K 3468). Then, samples were dehydrated (70%, 80%, 90%, 2× 100% ethanol, 3× Xylol; 30 s each).

Nestin fluorescent staining was performed as follows: unmasking the antigens with citrate buffer pH 6.0 (DAKO S2369) at 95ºC for 1hour ; blocking with Normal Goat Serum (1:10; DAKO X0907), for 1 hour, incubation of mouse-anti-human nestin (1:200; Chemicon Int) for 1 hour, and incubation with the secondary antibody Alexa Flour® goat-anti-mouse 488 (1:500) for 1h. Finally, samples were stained with DAPI and mounted.

Potential non-specific binding of secondary antibodies was assessed by omission primary antibodies in sections that were otherwise treated in a similar manner. Also, the specifity of the primary antibodies were confirmed by the use of isotype controls.

We have previously worked using the antibodies included in the present study in many other research works, on formalin-fixed tissues from either stillborn or aborted human fetuses and from adults, as well as on cell cultures of rat and human enteric neurospheres (Rauch et al. 2006; Hagl et al. 2013a; Hagl et al. 2013b; Schafer et al. 2003). The specificity of the Picrosirius red staining antibody has been tested on the human and rat tissues by (Yu et al. 2017; Lattouf et al. 2014). The specificity of Smooth Muscle Actin (B4) antibody (Santa Cruz Biotechnology, sc-53142), has been tested on rat and human tissues and cells by immunofluorescence analysis (Breikaa et al. 2013; Tian et al. 2015).

Image analysis and measurements of animal samples

The diameter of the small bowel and thickness of the muscle layers were measured. The thickness of muscle layers was measured each 500 µm in the pre-anastomotic small intestine (jejunum) and the post-anastomotic intestine (Ileum) in the rSBS–group and in control-group. Both the bowel's diameter and thickness of muscle layers impact the amount of muscle tissue in the bowel. Thus, the “Area of muscle circumference” was counted according to the formula: Area of muscle circumference = (π x diameter) x thickness of muscle layers.

Nestin-peroxide stained samples were subjected to morphometric analysis to analyze the quantity of nestin-stained myenteric ganglia and nestin-positive areas in muscle layers in a whole crosscut section (in bowel circumference).

We used an nestin-immunofluorescence staining to analyze nestin-positive areas within single myenteric ganglion. The myenteric plexus was identified, and the ratio of nestin-positive area to the total area of myenteric plexus was calculated.

Finally, to determine whether the changes in thickness of the muscle layers of the bowel were due to hypertrophy or hyperplasia, we analyzed the morphology, size and number of the nuclei in the different bowel muscle layers (circular and longitudinal) using the ImageJ Software (Version: 1.53a, USA). Based on the DAPI channel pictures, the areas of the circular (CML) and longitudinal muscle (LML) layers were selected and isolated. Then, the individual layers were separated, thresholded, binarized, the background was removed, despeckled, watershed, and finally the exactly individual nuclei shapes selected, measured and analyzed with the software (Fig. 1). In total, for the control groups for the orally (proximal) and anally (distal) samples, at leats 6 samples (and 5–6 pictures/sample) were quantified. For the SBS (KD) sections, at least 6 samples (and 3–6 pictures/sample) were analyzed for the oral (proximal) segments, while at least 5 samples (and3-8 pictures/samples) were quantified for the anally (distal) part.

Human samples

Human samples were collected according to the approval of the local ethic committee (2016-525N-MA) of the Medical Faculty Mannheim University of Heidelberg. In this study, no bowel resections for research purposes took place. Only resections for medical indications were used.

We conducted a comparative analysis of pathomorphological changes in minor resections of the small bowel, fulfillment of which were medically required during the surgical treatment of children with SBS (4 patients), which made up the main group.

The control group was composed of patients who underwent resection of minor small bowel segments because of the medical indication: in Meckel's diverticulum (n = 3) and in one case of foreign body, causing intestinal obstruction with the need of minor resection. None of the patients in the control group had SBS neither intestinal failure.

The patients were age-matched: the age ranged from 4 months to 7.5 years in patients with SBS and from 4 months to 10.5 years in the control group. The main and the control group had an identical gender composition: one boy and three girls.

Staining and microscopy of human samples

After removing the tissue from the patient, the specimens were transferred directly from surgery to the laboratory, fixed in 4% paraformaldehyde overnight, embedded in paraffin and sectioned at 4 µm thickness. Then, samples were dehydrated (70%, 80%, 90%, 2× 100% ethanol, 3× Neo-Clear; 30 s each), incubated in the steamer with citrate buffer pH 6.0 (DCS CL009C-100) for 45 min., following an enzymatic unmasking with Protease K (DAKO Agilent S3020) for 8 min. at 95ºC. Next, samples were permeabilized with 0.5% Triton X100, and blocked with Normal Alpaca Serum (Jackson ImmunoResearch Laboratories, Inc.) for 1h and then incubated with the corresponding primary antibodies: mouse-anti-human nestin (1:100; Millipore MAB 5326) and rabbit-anti-PGP9.5 (1:250; DAKO Agilent Z5116) for 1h at room temperature. The Negative-Control was incubated with Tris-Phosphat-Buffer + 0.5% TWEEN 20. After 3 washes in PBS-Tween, samples were incubated for 1h with the corresponding secondary antibodies: Alexa Fluor® alpaca-anti-rabbit 594 nm (1:500), Alexa Fluor® alpaca-anti-mouse 488 nm (1:500) (Jackson ImmunoResearch Laboratories, Inc.). Regarding nuclear staining, slides were either shortly incubated with DAPI (4',6-Diamidin-2-phenylindol, Dihydrochlorid) (Thermo Fisher 65-0880-92) and DAKO Fluorescence Mounting Media (DAKO Agilent S302380), or covered up directly with Roti®MOUNT Fluore Care DAPI (Carl Roth HP20.1).

Image acquisition

Pictures were taken with the light and fluorescence inverted microscope Keyence BZ-9000E, (KEYENCE CORPORATION, Higashi-Nakajima, Higashi-Yodogawa-ku, Osaka, 533–8555 1, Japan), using the objectives: 20X (Nicon Plan Apo, 20X/0.75, DIC N2 OFN25 WD 1.0) and 40X (Nicon Plan Apo, 40X/0.95, DIC M/N2 OFN25 WD 0.14). All pictures were acquired and processed with the Keyence camera and software. The camera is installed in the Keyence BZ-9000E microscope (2/3 inch, 1,5 millions Pixel monochromer CCD Fotosensor (with LC Filter)) with shooting condition 1360x1024 pixel. The acquisition software is delivered with the Keyence BZ-9000E microscope: Program “BZ-II Viewer” (Version: 2.1.00a0.0100.0101.0100.0003). Image acquisition was performed in the following conditions: detector gain + 12dB, bit depth 24, fluorescence filters OP-66834 BZ Filter DAPI-BP (excitation wavelength 360/40 nm, absorption wavelength 460/50 nm), OP-66836 BZ Filter GFP-BP (excitation wavelength 470/40 nm, cold mirror wavelength 505 nm, absorption wavelength 535/50 nm), OP-66838 BZ Filter TexasRed (excitation wavelength 560/40 nm, absorption wavelength 630/60 nm), excitation time 1/15 – 1/90 sec.; multifluorescence image acquisitions were performed successively. The obtained pictures were analysed using the “BZ-II Analyser” (Version: 2.1) software, which is delivered with the Keyence BZ-9000E microscope.

Statistical analysis

Statistics were performed with the JMP Software. Data distribution was determined using the Shapiro-Wilk test and visual analysis. Since the data does not fit a normal distribution, nonparametric statistics were used. Additional to mean und standard deviation, the median and the twenty-fifth and seventy-fifth percentile were calculated. The description in the text for normal distribution of the data: “Mean ± Standard Deviation”, for non-normal distribution of the data: "Median (25th Percentile − 75th Percentile)". Analysis and comparison for quantitative analysis were performed using the Student T-test for normal distribution and the Wilcoxon test for not normal distribution. For qualitative attributes, Fisher's exact and Chi-square tests were used. Statistical significance was accepted when the p-value was 0.05 or less (*$p < 0.05$). Nonparametric correlations were performed with the Spearmen's correlation test.

Results

The muscle layers is thickened in SBS

In order to investigate the intestinal adaptation of the muscle-neuronal complex, we analyzed the smooth muscle morphology after small bowel resection. To do so thickness of longitudinal and circular muscle layers and length and diameter of the intestine were measured.

The rats with short bowel resection showed significant increace of the thickness of smooth muscle layer and small intestinal dilatation compared to controls (Fig. 2a,b).

Also the thickness of the muscle layer of the small bowel significantly increased in the rSBS group in both jejunum (76 µm (42 µm- 135 µm)) and ileum (53 µm (36 µm – 74 µm)) compared to the control group in jejunum (35.3 µm (26.25 µm – 51.75 µm) $p < 0.0001$) and ileum (42 µm (30 µm – 62 µm). $p < 0.0001$) (Fig. 2c).

To determine which compartment or cell type contributes in increasing the thickness of the muscle layer in SBS gut sections were stained with antibodies against smooth muscle actin to identify and quantify the amount of smooth muscle cells. Picrosirius red staining identified the connective tissue (collagen I and III). Figure 3 shows, that in rSBS group there is no significant increase of connective tissue (collagen I and III) in the muscle layer (Fig. 3a,b) in comparison to the control group, and in the same group the proliferation of the muscle cells is clearly vivible (Fig. 3c,d).

Next, we measured the diameter of the small bowel. The rSBS group showed a significant increase in both jejunum (7573 µm (6428 µm – 8334 µm), $p < 0.0001$) and ileum (6020 µm (4837 µm – 6706 µm), $p < 0.0012$) in comparison to the control group (jejunum 4128 µm (377 µm – 4511 µm) ; ileum 4757 µm (4405 µm – 5134 µm)).

Increased muscle thickness and the small bowel diameter in rSBS lead to an amplified quantity of muscle tissue in the intestinal muscle layers. The area of muscle tissue was measured by calculating the “Area of muscle circumference” of the small bowel, as described above in materials and methods. The area of muscle circumference in the rSBS group was significantly increased in jejunum (2221225 μm^2 (1050679 μm^2 – 83725212 μm^2), $p < 0.05$) as well as in the ileum (11161352 μm^2 (843239 μm^2- 1503000 μm^2), $p < 0.05$) compared to the control (jejunum 466928 μm^2 (370783 μm^2 – 587079 μm^2), ileum 703396 μm^2 (502434 μm^2 – 1023298 μm^2) (Fig. 4).

The next aspect of our study was to evaluate whether the increase in the volume of muscle tissue of the small intestine in SBS is the result of hypertrophy or hyperplasia of muscle tissue. For this, we carried out a morphometric analysis of nuclei (size and density) of muscle cells of the bowel wall. The analysis showed that in SBS, the size of the nuclei (area) is significantly increased in comparison with the control group in both the longitudinal and circular muscle layers, and in the jejunum, and in the ileum (Table 1, Fig. 5).

Table 1
Size of the nuclei (the area of the nucleus in the cross section) (rat).

Part of the bowel	Muscle layer	Group	Minimum	25th percentile	Median	75th percentile	Maximum	P Wilcoxon
Ileum	Circular	Control	1.012	17.578	27.966	40.88275	255.67	< 0.0001
		rSBS	1.084	21.607	34.289	52.752	196.27	
	Longitudinal	Control	1.012	7.949	12.429	18.066	103.99	< 0.0001
		rSBS	1.012	8.527	13.947	21.462	117.79	
Jejunum	Circular	Control	1.156	17.126	27.388	39.18425	117.79	< 0.0001
		rSBS	1.156	26.954	42.057	61.279	178.85	
	Longitudinal	Control	1.012	7.082	11.345	17.343	73.925	< 0.0001
		rSBS	1.012	11.49	18.572	26.882	89.1	

However, the number of nuclei in 1000 μm^2 of the area by SBS is significantly smaller compared with the control group in both the longitudinal and transverse muscle layers, and the jejunum (before the anastomosis) and the ileum (after anastomosis) (Table 2, Fig. 6).

Table 2
Number of nuclei in 1000 μm^2 of the area of muscle layer (rat).

Part of the bowel	Muscle layer	Group	Minimum	25th percentile	Median	75th percentile	Maximum	P Wilcoxon
Ileum	Circular	Control	0	4.278	5.153	6.489	8.012	< 0.0001
		rSBS	2.300	2.625	2.959	3.970	5.906	
	Longitudinal	Control	7.776	9.152	10.440	11.147	12.994	< 0.0001
		rSBS	3.973	4.853	5.842	7.457	10.875	
Jejunum	Circular	Control	4.106	5.001	6.131	7.286	8.256	< 0.0001
		rSBS	2.789	2.893	3.605	4.608	5.324	
	Longitudinal	Control	9.238	10.213	10.855	13.489	14.736	< 0.0001
		rSBS	4.830	5.006	6.387	7.278	8.526	

Altogether, we can conclude that by SBS, the nuclei of the cells become larger, but the density of nuclei is lower, which indicates hypertrophy of both the nuclei and the muscle cells themselves.

These results indicate that in the case of a SBS, muscle tissue increases significantly in both parts of the small bowel, jejunum, and ileum, which manifests in an increased muscle thickness and an enlarged diameter of the small bowel. So, the leading pathophysiological mechanism of these changes is hypertrophy.

SBS samples contain more neuronal stem cells in ganglion of myenteric plexus

To explore the role of neurogenesis in intestinal adaptation in SBS, we performed nestin stainings (Fig. 7). Initially, we analyzed amount of myenteric ganglia with the nestin expression in the whole crosscut section (in bowel circumference) to identify whether the amount of myenteric ganglia with upregulatied of neuronal stem cells increase in SBS condition. For these purposes, we used nestin peroxidase staining and quantified the amount nestin-positive myenteric ganglia pro section (in bowel circumference).

The analysis revealed that the quantity of nestin-positive myenteric ganglia was significantly increased in the rSBS group compared to control in both parts of the small bowel: in the jejunum ($p<0.0001$) and ileum ($p<0.0001$). The number of nestin-positive myenteric ganglia by rSBS group in the jejunum was 8.5 (2–33.25) plexus, in the control group – 0 (0–1) plexus; in the ileum by rSBS group was 5.66 (1–9.25) plexus, by control group – 0 (0–0.75) plexus.

In SBS, a significantly higher number of ganglia in myenteric plexus with upregulated stem cells population was observed in jejunum and ileum compared to the control. These results suggest that in an effort to adapt to SBS, the myenteric plexus of jejunum and ileum respond with an increase of numer fo myenteric ganglia with neuronal stem cells.

Next, we analyzed the espression of nestin in the myenteric ganglia (Fig. 8a, b, c, d) by immunofluorescence.

Then, we calcultated the percentage of nestin-positive areas to the total area of the myenteric ganglia. Statistical analysis showed a significantly larger nestin-positive area in myenteric plexus in rSBS group compared to controls (jejunum: $p = 0.0125$, ileum: $p < 0.0001$) Thus, the percentage of nestin-positive area to the total area of the myenteric plexus in rats with SBS was in the jejunum was 3.36% (1.2% – 10.32%), in the ileum — 5.51% (2.14% – 8.17%); in rats of the control group in the jejunum —1.37% (0.42% – 3.25%) and in the ileum — 0.88% (0.31% – 2.44%) (Fig. 8e).

In SBS, a significantly higher neuronal stem cells population inside the ganglia in myenteric plexus was observed in jejunum and ileum compared to the control. These results suggest that in an effort to adapt to SBS, the myenteric plexus of jejunum and ileum respond with an increase of neuronal stem cells within the ganglia.

Altogether, given that neuronal stem cells are a source of new neurons, our results show that neurogenesis is significantly amplified in the whole small intestine to compensate the SBS condition.

There are more nestin-positive areas in intestinal muscle layers of the rats with SBS

Nestin peroxidase stained samples (Fig. 7) were analyzed and divided into two groups: 1) samples with a high nestin-positive areas in the muscle layers; 2) samples with a low or absent nestin-positive areas in the muscle layers.

In the rSBS group, the ratio of samples with a high nestin-positive areas was 85.7% (jejunum, $p < 0.05$) and 64.3% (ileum, $p < 0.05$), whereas in controls, high nestin-positive areas occurred only in 4.3% (jejunum) and 12.5% (ileum) respectively.

Thus, rSBS presents an accumulation of nestin in the myenteric plexus.

Nestin expression correlates with muscle hypertrophy

The size of muscle tissue inside the muscle layers (the area of muscle circumference) is an objective indicator of changes in muscle tissue during intestinal adaptation, because it evaluates both the intestinal diameter and the thickness of the muscular layers. Here we observed a moderate correlation between the bowel diameter and the thickness of the muscle layers ($r = 0.5447$, $p = 0.0001$) with the Spearmen's test. Besides, there was a strong positive correlation between the nestin-positive myenteric plexus and the size of muscle tissue in the muscle layers (the area of muscle circumference) ($r = 0.7524$, $p < 0.0001$) (Fig. 9).

Furthermore, the number of nestin-positive cells in muscle layers and the area of muscle circumference showed a significant positive correlation ($r = 0.7597$, $p < 0.0001$) (Fig. 9). The comparison between the quantity of nestin-positive myenteric plexus and the nestin-positive cells in muscle layers also presented a very positive correlation ($r = 0.8065$, $p < 0.0001$) (Fig. 9).

Altogether, there is an association between muscle hypertrophy, the rise of stem cells in muscle layers, and neurogenesis in myenteric plexus in the process of intestinal adaptation to SBS.

Human Data

To investigate whether a similar effect is seen in patients, we examined small bowel tissue samples from patients with and without SBS. In all cases, the small bowel resections were medically indicated. The specimens were first stained using Hematoxilin-eosin to verify the morphology of the myenteric plexus and select the most appropriate sites of the tissue for immunohistochemical staining (Fig. 10). Then, samples were co-stained with antibodies against both PGP 9.5 (a neuronal marker) and nestin (a neuronal precursor marker). This procedure allowed to observe nerve cells and neuronal stem cells in the samples, to assess the area that these cells occupy in the myenteric plexus (Fig. 10a, b) and to determine the arrangement of these two types of cells (Fig. 10c). Using the microscope software from Keyence BM9000X (Keyence), we mapped the myenteric plexus and quantified the proportion of nestin-positive areas (for neuronal stem cells) and PGP 9.5-positive areas (for neurons) (Fig. 10d).

Results showed a significant increase of neuronal stem cells in patients with SBS in comparison to healthy controls (Wilcoxon Test $p < 0.0001$). The observed proportion of stem cells in patients with SBS was $21.3 \pm 12.34\%$ of the total area of the myenteric plexus, whereas in the control group it was $6.8 \pm 3.98\%$. Thus, the proportion of stem cells in the myenteric plexus of SBS patients duplicates the number of the healthy control group (Fig. 10e).

On the other hand, the observed proportion of neuronal cells in the myenteric plexus in patients with SBS did not significantly differ from patients in the control group. However, the ratio of the proportion of stem cells to the proportion of neurons in the myenteric plexus increased significantly (Wilcoxon Test $p < 0.0001$). In patients with SBS this indicator was $0.71\% \pm 0.66\%$ and in the control group — $0.24 \pm 0.16\%$ (Fig. 10f).

In summary, we observe a constant proportion of neurons, but an increase of neuronal precursor cells in the myenteric plexus, which suggest that the adaptation to SBS presents an expansion of the plexus.

Discussion

During the last years, changes in muscle layers after massive small bowel resection have been controversially discussed. While several authors described a hypertrophy of intestinal muscle layers as a result of intestinal

adaptation in SBS experiments on rats (Chen et al. 2012; Chen et al. 2015; Chen et al. 2013), others did not find evidence for a hypertrophy of the muscle layers (Martin et al. 2008).

Despite the fact that the ENS is crucial for bowel motility and its tighty connected to intestinal smooth muscles (Lotfollahzadeh et al. 2021), the changes in ENS after massive small bowel resection have not been published yet.

Here in this study we have analyzed the intestinal muscle layers and the ENS together as a neuro-muscular complex. In order to assess the plasticity of the ENS (Schafer et al. 2009) in the intestinal adaptation to SBS, we used nestin, a well-known ENS precursor cell marker (Vanderwinden et al, 2002(Grundmann et al. 2016), (Kulkarni et al. 2017), in both rats and humans samples after massive small bowel resection.

Our results show that the thickness of the small bowel muscle wall significantly increased in the SBS group in both proximal and distal segments. Many previous published human data on morphological changes of the small bowel in SBS was only focused on the mucosal layer (Tappenden 2014c, b; Doldi 1991; McDuffie et al. 2011; Joly et al. 2009). Besides, while previous studies, explored the changes in the muscle layers mainly in the proximal part (in the jejunum, proximal to the resection site) (Martin et al. 2008; Chen et al. 2012; Chen et al. 2015; Chen et al. 2013), here we have analyzed also the intestine distal parts (in the ileum, distal to the resection site), thus we can state that muscle hypertrophy occurs in both jejunum and ileum. Also the “Area of muscle circumference” in the SBS group was significantly increased in jejunum, as well as in the ileum compared to the healthy control group.

Altogether we demonstrated that muscle tissue increases significantly in both parts of the small bowel, jejunum and ileum, which results in an increased muscle thickness and an enlarged small bowel diameter .

We also evaluated whether the morphological changes in the muscle layers were a result of hypertrophy or hyperplasia. For that, a morphometric analysis of nuclei (size and density) of the muscle cells was performed. Our data revealed that in SBS, the nuclei of the muscle cells became bigger, but the density of nuclei was reduced, indicating that the leading pathophysiological mechanism of these changes is hypertrophy, which is supported by previous studies (Chen et al. 2015).

In all, our observations indicate that following massive small bowel resection, the intestine responds developing muscle hypertrophy in an effort to re-adapt itself to the new situation, where absortive capacity is strongly reduced.

Concerning the ENS plasticity, we found a higher nestin expression in the myenteric plexus in the remaining small bowel of the SBS samples, which demonstrates that not only the muscle wall but also the ENS responds to bowel resection as part of the adaptation process. These results point to a regenerative potential and plasticity of the ENS in the intestinal adjustment to SBS. Actually, a participation of the ENS in the intestinal epithelial growth and repair after SBS has previously been suggested (Toumi et al. 2003), (Haxhija et al. 2007).

Nestin expression was also detected in endothelial cells of newly formed blood vessels (Matsuda et al. 2013) and myofibroblasts (Beguin et al. 2012), demonstrating the regenerative character of nestin expression. So the higher number of nestin-expressing cells in the muscle layers that we found, could suggest that also complementary neuronal progenitor cells outside of myenteric plexus (ganglia) are stimulated during intestinal adaptation.

However, the nestin expression detected in SBS samples within the muscle layers was comparable to that observed in the myenteric plexus. This could point to an intensified influence of the ENS within the smooth muscle layers and intrinsic activation of neural precursors. It is discussed that after 5-HT4 activation, newly born neurons appeared in extra-ganglionic locations and migrated into MP (Liu et al. 2009). Thus, the ENS may execute a more substantial

influence and intrinsic activation of neural precursors on the smooth muscle layers, as was previously suggested (Birbrair et al. 2013). Furthermore, the enteric neurons inside the myenteric plexus (ganglia) and neural precursors on the smooth muscle layers could activate or enhance the proliferation of the muscle cells.

In conclusion, our results show an upregulation of nestin in SBS and evidence that the ENS activates its neurogenic potential and participates in intestinal adaptation.

Moreover, we showed that smooth muscle hypertrophy has a strong positive correlation with the activation of nestin-positive cells in the myenteric plexus ($r = 0.7524$, $p < 0.0001$), as well as in muscle layers ($r = 0.8065$, $p < 0.0001$). A pronounced positive correlation between the proportion of stem cells in the myenteric plexus and smooth muscle hypertrophy allows us to consider the muscle layers of the small intestine and the ENS as a single neuromuscular complex, which plays an essential role in the functioning of the small intestine.

In summary, we have identified several readjustments in the gut following SBS, such us an increase in the diameter of the small intestine, hypertrophy of the small intestine muscle layers, and an increase in the proportion of neuronal stem cells in both the myenteric plexus (ganglia) and the small intestine muscle layers. These observations represent the most important pathophysiological mechanisms in SBS and occur in patients with this pathology. Finally, all these changes induce dilated areas of small bowel with muscular wall hypertrophy.

From a clinical point of view, this phenomenon suggests that the diameter of the small intestine must be measured regularly in patients with SBS. This step will make possible a timely recognition of the small bowel dilatation and the development of intestinal congestion, as well as enable future indications for intestinal lengthening surgeries in a prompt manner.

In conclusion, smooth muscle hypertrophy and neuroplasticity characterize the intestinal re-adaptation in SBS. The ENS activates its neurogenic potential through the neural stem cells and thereby participates in the intestinal adaptation. This process is tightly correlated with an increased expression of neural precursors in the ENS and an increase of the muscle tissue in muscle layers. Since the mechanism of intestinal adaptation is complex and the role of the ENS comprises neural stem cell regulation, further research on enteric glial and neuronal cells is necessary to elucidate the role of enteric neural stem cells in this process.

Declarations

ACKNOWLEDGEMENTS

We would like to thank Sabine Heumüller-Klug und Elvira Wink for brilliant advices and excellent assistance.

Data availability

The datasets generated and analysed during the current study are available from the corresponding author on reasonable request.

CONFLICT OF INTEREST

None to declare.

References

1. Beguin PC, Gosselin H, Mamarbachi M, Calderone A (2012) Nestin expression is lost in ventricular fibroblasts during postnatal development of the rat heart and re-expressed in scar myofibroblasts. J Cell Physiol 227 (2):813–820. doi:10.1002/jcp.22794
2. Birbrair A, Zhang T, Wang ZM, Messi ML, Enikolopov GN, Mintz A, Delbono O (2013) Skeletal muscle neural progenitor cells exhibit properties of NG2-glia. Experimental cell research 319 (1):45–63. doi:10.1016/j.yexcr.2012.09.008
3. Breikaa RM, Algandaby MM, El-Demerdash E, Abdel-Naim AB (2013) Multimechanistic antifibrotic effect of biochanin a in rats: implications of proinflammatory and profibrogenic mediators. PLoS One 8 (7):e69276. doi:10.1371/journal.pone.0069276
4. Chen J, Du L, Xiao YT, Cai W (2013) Disruption of interstitial cells of Cajal networks after massive small bowel resection. World journal of gastroenterology: WJG 19 (22):3415–3422. doi:10.3748/wjg.v19.i22.3415
5. Chen J, Qin Z, Shan H, Xiao Y, Cai W (2015) Early Adaptation of Small Intestine After Massive Small Bowel Resection in Rats. Iran J Pediatr 25 (4):e530. doi:10.5812/ijp.530
6. Chen J, Wen J, Cai W (2012) Smooth muscle adaptation and recovery of contractility after massive small bowel resection in rats. Exp Biol Med (Maywood) 237 (5):578–584. doi:10.1258/ebm.2012.011338
7. Collins SM, Hurst SM, Main C, Stanley E, Khan I, Blennerhassett P, Swain M (1992) Effect of inflammation of enteric nerves. Cytokine-induced changes in neurotransmitter content and release. Ann N Y Acad Sci 664:415–424
8. Doldi SB (1991) Intestinal adaptation following jejuno-ileal bypass. Clin Nutr 10 (3):138–145. doi:10.1016/0261-5614(91)90049-i
9. Fichter M, Klotz M, Hirschberg DL, Waldura B, Schofer O, Ehnert S, Schwarz LK, Ginneken CV, Schafer KH (2011) Breast milk contains relevant neurotrophic factors and cytokines for enteric nervous system development. Molecular nutrition & food research 55 (10):1592–1596. doi:10.1002/mnfr.201100124
10. Fleming MA, 2nd, Ehsan L, Moore SR, Levin DE (2020) The Enteric Nervous System and Its Emerging Role as a Therapeutic Target. Gastroenterol Res Pract 2020:8024171. doi:10.1155/2020/8024171
11. Furness JB (2012) The enteric nervous system and neurogastroenterology. Nat Rev Gastroenterol Hepatol 9 (5):286–294. doi:10.1038/nrgastro.2012.32
12. Garcia SB, Kawasaky MC, Silva JC, Garcia-Rodrigues AC, Borelli-Bovo TJ, Iglesias AC, Zucoloto S (1999) Intrinsic myenteric denervation: a new model to increase the intestinal absorptive surface in short-bowel syndrome. J Surg Res 85 (2):200–203. doi:10.1006/jsre.1999.5670
13. Goulet O, Sauvat F (2006) Short bowel syndrome and intestinal transplantation in children. Current opinion in clinical nutrition and metabolic care 9 (3):304–313. doi:10.1097/01.mco.0000222116.68912.fc
14. Grundmann D, Markwart F, Scheller A, Kirchhoff F, Schafer KH (2016) Phenotype and distribution pattern of nestin-GFP-expressing cells in murine myenteric plexus. Cell and tissue research 366 (3):573–586. doi:10.1007/s00441-016-2476-9
15. Hagl CI, Heumuller-Klug S, Wink E, Wessel L, Schafer KH (2013a) The human gastrointestinal tract, a potential autologous neural stem cell source. PLoS One 8 (9):e72948. doi:10.1371/journal.pone.0072948
16. Hagl CI, Wink E, Scherf S, Heumuller-Klug S, Hausott B, Schafer KH (2013b) FGF2 deficit during development leads to specific neuronal cell loss in the enteric nervous system. Histochem Cell Biol 139 (1):47–57. doi:10.1007/s00418-012-1023-3

17. Haxhija EQ, Yang H, Spencer AU, Sun X, Teitelbaum DH (2007) Intestinal epithelial cell proliferation is dependent on the site of massive small bowel resection. Pediatric surgery international 23 (5):379–390. doi:10.1007/s00383-006-1855-9
18. Hitch MC, Leinicke JA, Wakeman D, Guo J, Erwin CR, Rowland KJ, Merrick EC, Heuckeroth RO, Warner BW (2012) Ret heterozygous mice have enhanced intestinal adaptation after massive small bowel resection. American journal of physiology Gastrointestinal and liver physiology 302 (10):G1143-1150. doi:10.1152/ajpgi.00296.2011
19. Ives GC, Demehri FR, Sanchez R, Barrett M, Gadepalli S, Teitelbaum DH (2016) Small Bowel Diameter in Short Bowel Syndrome as a Predictive Factor for Achieving Enteral Autonomy. The Journal of pediatrics 178:275–277 e271. doi:10.1016/j.jpeds.2016.08.007
20. Joly F, Mayeur C, Messing B, Lavergne-Slove A, Cazals-Hatem D, Noordine ML, Cherbuy C, Duee PH, Thomas M (2009) Morphological adaptation with preserved proliferation/transporter content in the colon of patients with short bowel syndrome. American journal of physiology Gastrointestinal and liver physiology 297 (1):G116-123. doi:10.1152/ajpgi.90657.2008
21. Kaunitz JD, Akiba Y (2019) Control of Intestinal Epithelial Proliferation and Differentiation: The Microbiome, Enteroendocrine L Cells, Telocytes, Enteric Nerves, and GLP, Too. Digestive diseases and sciences 64 (10):2709–2716. doi:10.1007/s10620-019-05778-1
22. Kulkarni S, Micci MA, Leser J, Shin C, Tang SC, Fu YY, Liu L, Li Q, Saha M, Li C, Enikolopov G, Becker L, Rakhilin N, Anderson M, Shen X, Dong X, Butte MJ, Song H, Southard-Smith EM, Kapur RP, Bogunovic M, Pasricha PJ (2017) Adult enteric nervous system in health is maintained by a dynamic balance between neuronal apoptosis and neurogenesis. Proceedings of the National Academy of Sciences of the United States of America 114 (18):E3709-e3718. doi:10.1073/pnas.1619406114
23. Lattouf R, Younes R, Lutomski D, Naaman N, Godeau G, Senni K, Changotade S (2014) Picrosirius red staining: a useful tool to appraise collagen networks in normal and pathological tissues. J Histochem Cytochem 62 (10):751–758. doi:10.1369/0022155414545787
24. Lei NY, Ma G, Zupekan T, Stark R, Puder M, Dunn JC (2011) Controlled release of vascular endothelial growth factor enhances intestinal adaptation in rats with extensive small intestinal resection. Surgery 150 (2):186–190. doi:10.1016/j.surg.2011.05.003
25. Lin S, Stoll B, Robinson J, Pastor JJ, Marini JC, Ipharraguerre IR, Hartmann B, Holst JJ, Cruz S, Lau P, Olutoye O, Fang Z, Burrin DG (2019) Differential action of TGR5 agonists on GLP-2 secretion and promotion of intestinal adaptation in a piglet short bowel model. American journal of physiology Gastrointestinal and liver physiology 316 (5):G641-G652. doi:10.1152/ajpgi.00360.2018
26. Liu MT, Kuan YH, Wang J, Hen R, Gershon MD (2009) 5-HT4 receptor-mediated neuroprotection and neurogenesis in the enteric nervous system of adult mice. The Journal of neuroscience: the official journal of the Society for Neuroscience 29 (31):9683–9699. doi:10.1523/jneurosci.1145-09.2009
27. Lotfollahzadeh S, Taherian M, Anand S (2021) Hirschsprung Disease. In: StatPearls. Treasure Island (FL),
28. Martin CA, Bernabe KQ, Taylor JA, Nair R, Paul RJ, Guo J, Erwin CR, Warner BW (2008) Resection-induced intestinal adaptation and the role of enteric smooth muscle. Journal of pediatric surgery 43 (6):1011–1017. doi:10.1016/j.jpedsurg.2008.02.015
29. Martin CA, Perrone EE, Longshore SW, Toste P, Bitter K, Nair R, Guo J, Erwin CR, Warner BW (2009) Intestinal resection induces angiogenesis within adapting intestinal villi. J Pediatr Surg 44 (6):1077–1082; discussion 1083. doi:10.1016/j.jpedsurg.2009.02.036

30. Matsuda Y, Hagio M, Ishiwata T (2013) Nestin: a novel angiogenesis marker and possible target for tumor angiogenesis. World J Gastroenterol 19 (1):42–48. doi:10.3748/wjg.v19.i1.42
31. McDuffie LA, Bucher BT, Erwin CR, Wakeman D, White FV, Warner BW (2011) Intestinal adaptation after small bowel resection in human infants. Journal of pediatric surgery 46 (6):1045–1051. doi:10.1016/j.jpedsurg.2011.03.027
32. McMellen ME, Wakeman D, Longshore SW, McDuffie LA, Warner BW (2010) Growth factors: possible roles for clinical management of the short bowel syndrome. Seminars in pediatric surgery 19 (1):35–43. doi:10.1053/j.sempedsurg.2009.11.010
33. Niesler B, Kuerten S, Demir IE, Schafer KH (2021) Disorders of the enteric nervous system - a holistic view. Nat Rev Gastroenterol Hepatol 18 (6):393–410. doi:10.1038/s41575-020-00385-2
34. O'Brien DP, Nelson LA, Huang FS, Warner BW (2001) Intestinal adaptation: structure, function, and regulation. Seminars in pediatric surgery 10 (2):56–64
35. Oliveira C, de Silva N, Wales PW (2012) Five-year outcomes after serial transverse enteroplasty in children with short bowel syndrome. J Pediatr Surg 47 (5):931–937. doi:10.1016/j.jpedsurg.2012.01.049
36. Rauch U, Klotz M, Maas-Omlor S, Wink E, Hansgen A, Hagl C, Holland-Cunz S, Schafer KH (2006) Expression of intermediate filament proteins and neuronal markers in the human fetal gut. J Histochem Cytochem 54 (1):39–46. doi:10.1369/jhc.4A6495.2005
37. Schafer KH, Hagl CI, Rauch U (2003) Differentiation of neurospheres from the enteric nervous system. Pediatr Surg Int 19 (5):340–344. doi:10.1007/s00383-003-1007-4
38. Schafer KH, Van Ginneken C, Copray S (2009) Plasticity and neural stem cells in the enteric nervous system. Anatomical record (Hoboken, NJ: 2007) 292 (12):1940–1952. doi:10.1002/ar.21033
39. Stephens AN, Pereira-Fantini PM, Wilson G, Taylor RG, Rainczuk A, Meehan KL, Sourial M, Fuller PJ, Stanton PG, Robertson DM, Bines JE (2010) Proteomic analysis of the intestinal adaptation response reveals altered expression of fatty acid binding proteins following massive small bowel resection. Journal of proteome research 9 (3):1437–1449. doi:10.1021/pr900976f
40. Stern LE, Erwin CR, O'Brien DP, Huang F, Warner BW (2000) Epidermal growth factor is critical for intestinal adaptation following small bowel resection. Microscopy research and technique 51 (2):138–148. doi:10.1002/1097-0029(20001015)51:2<138::AID-JEMT5>3.0.CO;2-T
41. Sukhotnik I, Haj B, Pollak Y, Dorfman T, Bejar J, Matter I (2016) Effect of bowel resection on TLR signaling during intestinal adaptation in a rat model. Surgical endoscopy 30 (10):4416–4424. doi:10.1007/s00464-016-4760-x
42. Tappenden KA (2014a) Intestinal adaptation following resection. JPEN Journal of parenteral and enteral nutrition 38 (1 Suppl):23S-31S. doi:10.1177/0148607114525210
43. Tappenden KA (2014b) Intestinal Adaptation Following Resection. JPEN Journal of parenteral and enteral nutrition. doi:10.1177/0148607114525210
44. Tappenden KA (2014c) Pathophysiology of short bowel syndrome: considerations of resected and residual anatomy. JPEN Journal of parenteral and enteral nutrition 38 (1 Suppl):14S-22S. doi:10.1177/0148607113520005
45. Tian L, Chen K, Cao J, Han Z, Gao L, Wang Y, Fan Y, Wang C (2015) Galectin-3-induced oxidized low-density lipoprotein promotes the phenotypic transformation of vascular smooth muscle cells. Mol Med Rep 12 (4):4995–5002. doi:10.3892/mmr.2015.4075

46. Toumi F, Neunlist M, Cassagnau E, Parois S, Laboisse CL, Galmiche JP, Jarry A (2003) Human submucosal neurones regulate intestinal epithelial cell proliferation: evidence from a novel co-culture model. Neurogastroenterol Motil 15 (3):239–242. doi:409 [pii]
47. Vomhof-DeKrey EE, Lansing JT, Darland DC, Umthun J, Stover AD, Brown C, Basson MD (2021) Loss of Slfn3 induces a sex-dependent repair vulnerability after 50% bowel resection. American journal of physiology Gastrointestinal and liver physiology 320 (2):G136-G152. doi:10.1152/ajpgi.00344.2020
48. Weih S, Kessler M, Fonouni H, Golriz M, Hafezi M, Mehrabi A, Holland-Cunz S (2012) Current practice and future perspectives in the treatment of short bowel syndrome in children-a systematic review. Langenbeck's archives of surgery / Deutsche Gesellschaft fur Chirurgie 397 (7):1043–1051. doi:10.1007/s00423-011-0874-8
49. Wood JD (2004) Enteric neuroimmunophysiology and pathophysiology. Gastroenterology 127 (2):635–657
50. Yu X, Gong Z, Lin Q, Wang W, Liu S, Li S (2017) Denervation effectively aggravates rat experimental periodontitis. J Periodontal Res 52 (6):1011–1020. doi:10.1111/jre.12472

Figures

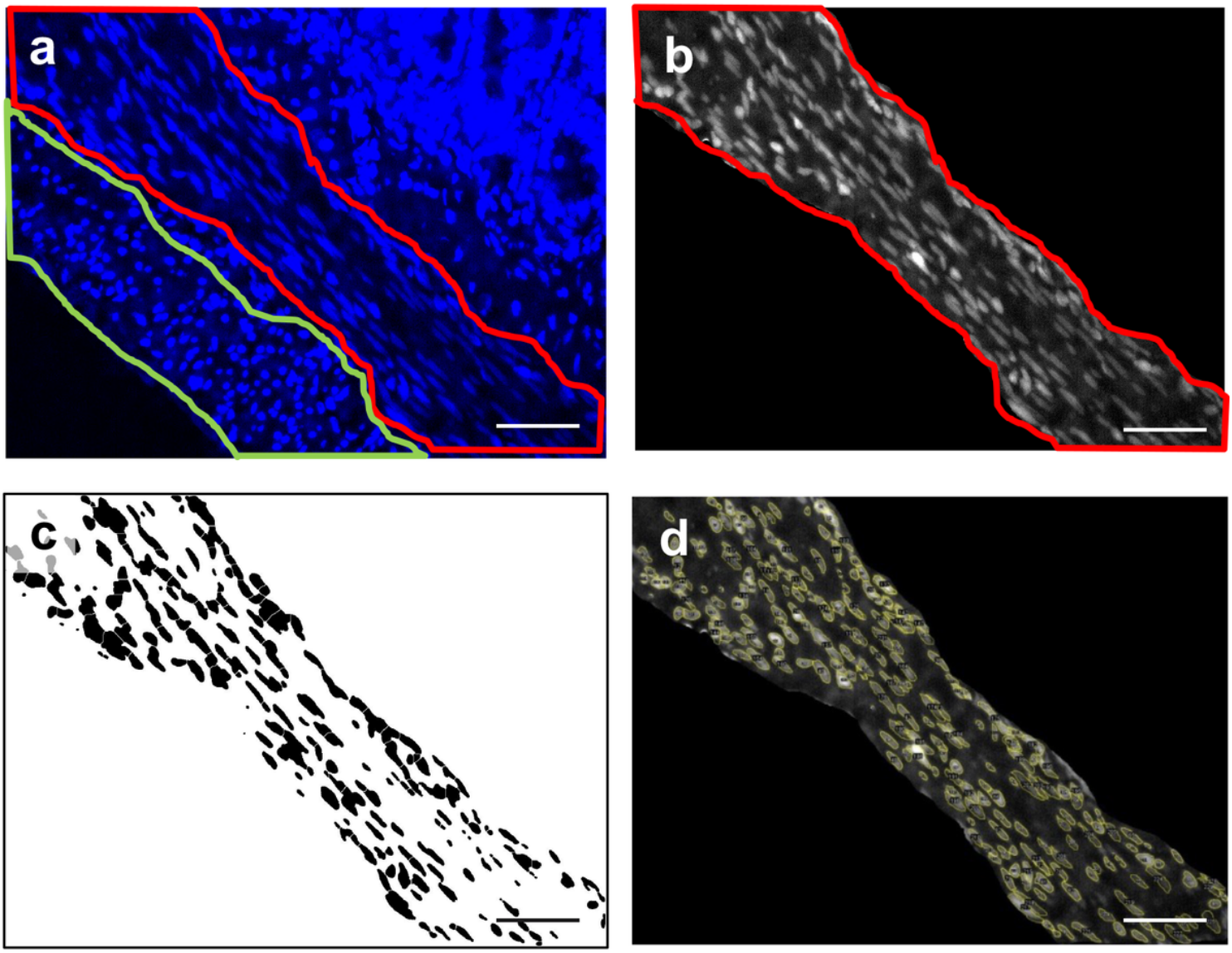

Figure 1

Process of nuclear analysis in the muscle layers of the small intestinal wall (rat). a- DAPI staining of nuclei. Areas of longitudinal (green) and circular (red) muscle were outlined. b- isolated circular muscle layer in 16 bit picture using ImageJ Software. c- Mapping of the picture B using ImageJ Software based on binary imaging. d- counting and analyzing of the circular muscle layer using ImageJ Software. Scale bar is 50 µm.

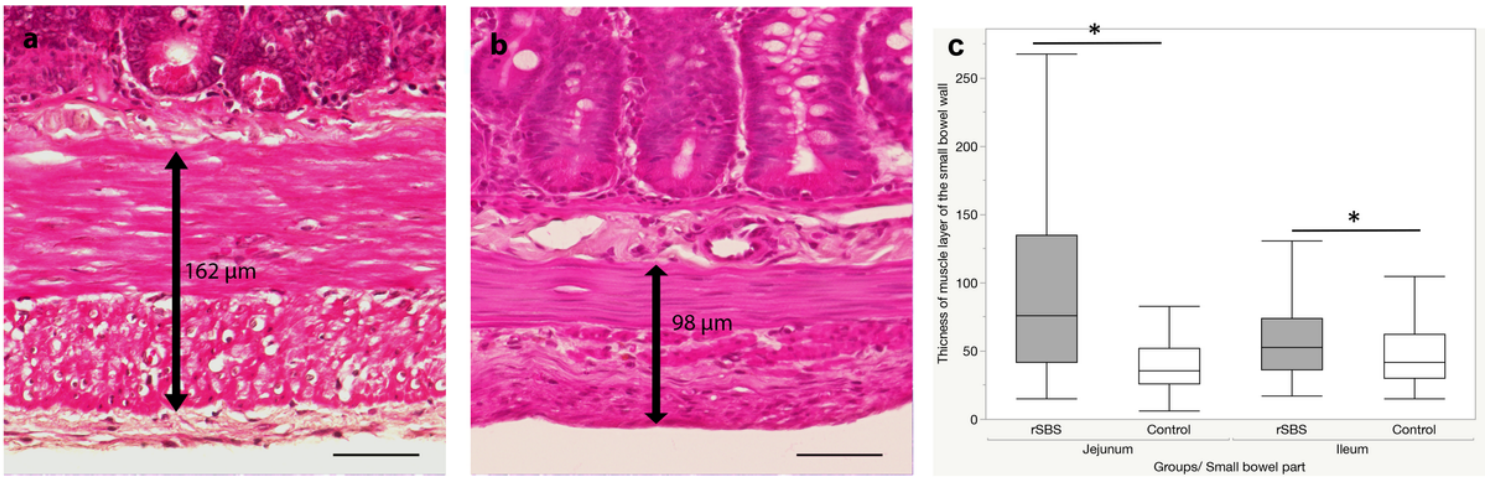

Figure 2

Haematoxylin-Eosin (HE) staining of control (a) and resected Short Bowel Syndrome (rSBS) (b) sections two weeks after surgery (rat). Arrows indicate the thickness of the muscle layer, c -thickness of small intestine muscle layer. The comparison between control (Control) and resected short bowel syndrome (rSBS) samples revealed a significant increase in the thickness of muscle layer in rSBS compared to control in jejunum and ileum. Values: median, the top and bottom of the box represent the seventy-fifth and twenty-fifth percentile. The whiskers indicate the maximum and minimum (not including outliers). Wilcoxon test: * p<0,0001. Scale bar is 50 µm.

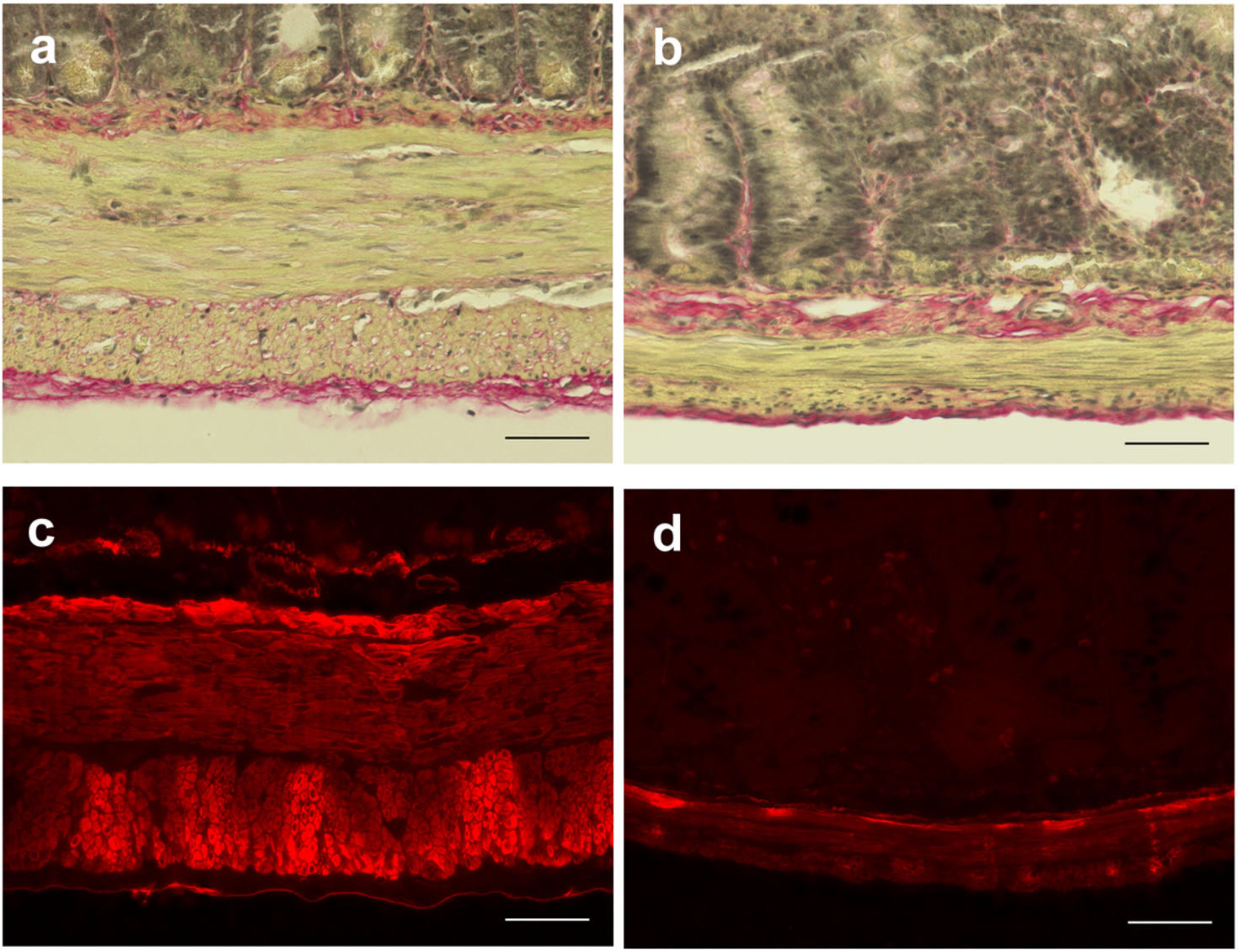

Figure 3

Section of small bowel wall stained with Picrosirius red and fluorescence staining with antibodies against smooth muscle actin (SMA) (rat): a- short bowel syndrome (rSBS) Picrosirius red staining , b– control group Picrosirius red staining, c– short bowel syndrome (rSBS) SMA staining, d – control group SMA staining. In Picrosirius red staining, collagen fibers have a red color. In SMA staining, smooth muscle cells present a fluorescence red color. Scale bar is 50 μm.

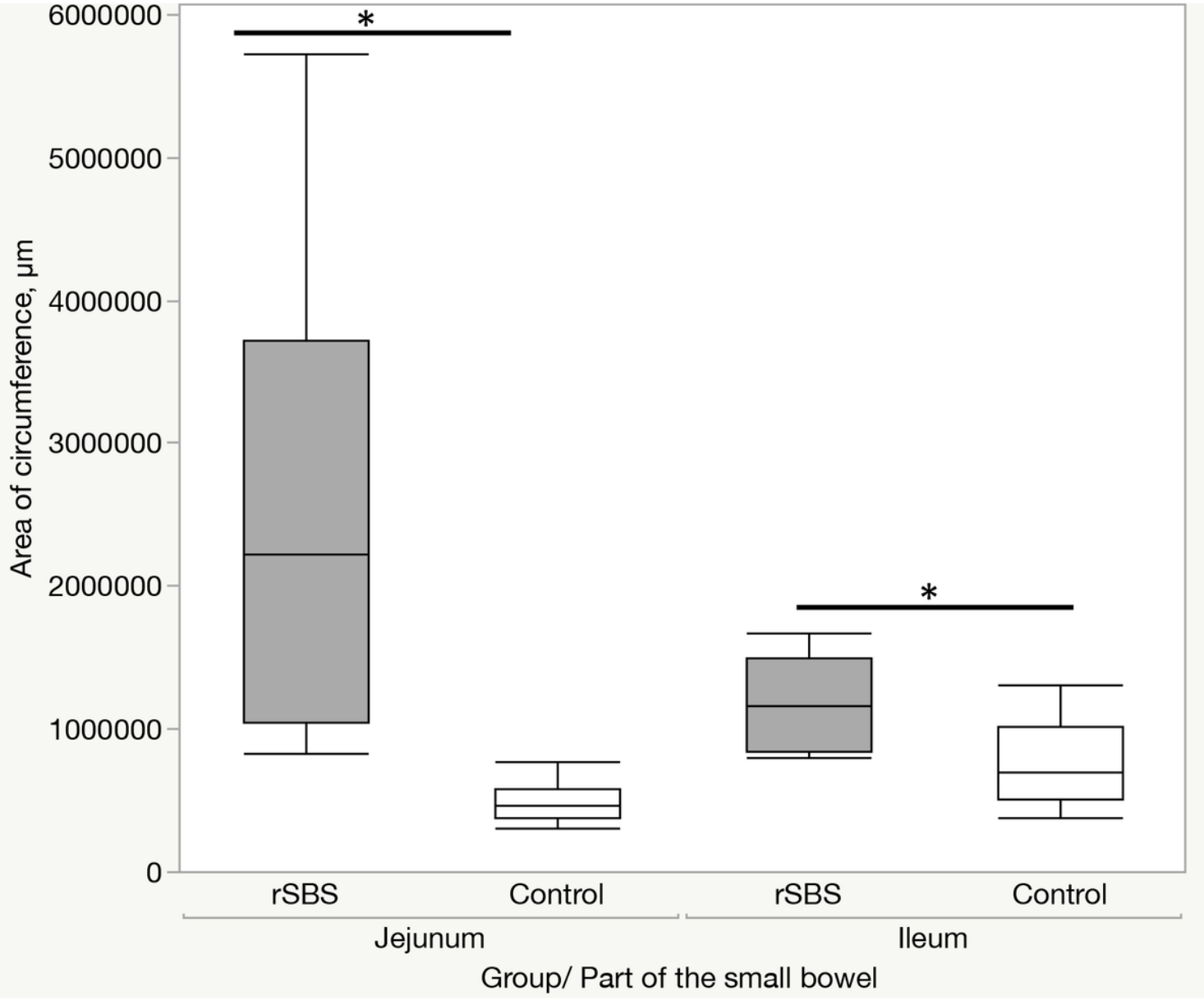

Figure 4

Area of muscle circumference of the small bowel (rat). The comparison between control (Control) and short bowel syndrome (rSBS) revealed a significant increase of the muscle circumference of the small bowel in rSBS compared to control in jejunum und ileum. Values: median, the top and bottom of the box represent the seventy-fifth and twenty-fifth percentile. The whiskers indicate the maximum and minimum (not including outliers). Wilcoxon test: * $p<0.05$.

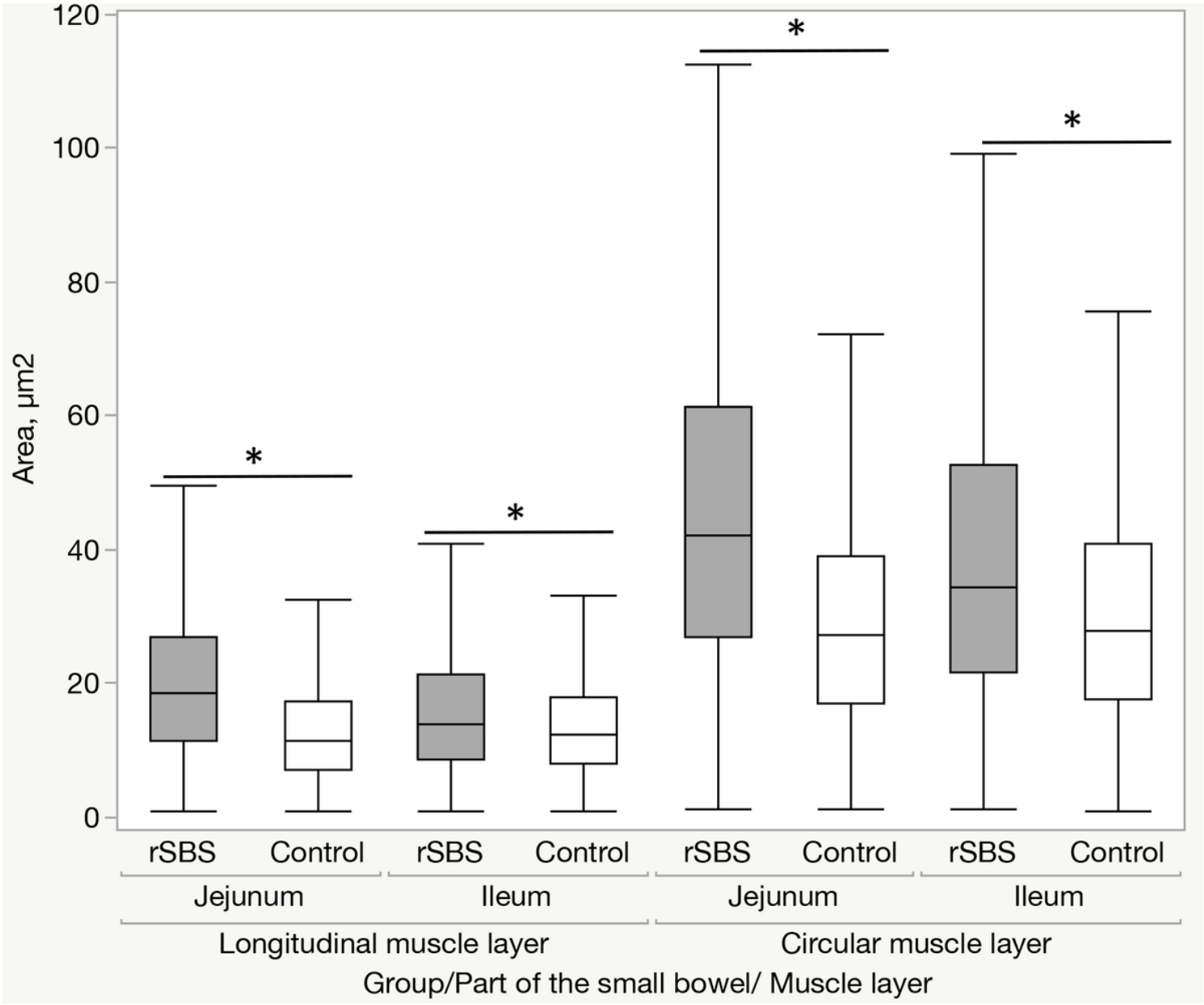

Figure 5

Size of the nuclei (area) (rat). The comparison between control (Control) and short bowel syndrome (rSBS) revealed a significant increase of the size of the nuclei in rSBS compared to control in jejunum und ileum. Values: median, the top and bottom of the box represent the seventy-fifth and twenty-fifth percentile. The whiskers indicate the maximum and minimum (not including outliers). Wilcoxon test: * p<0,0001.

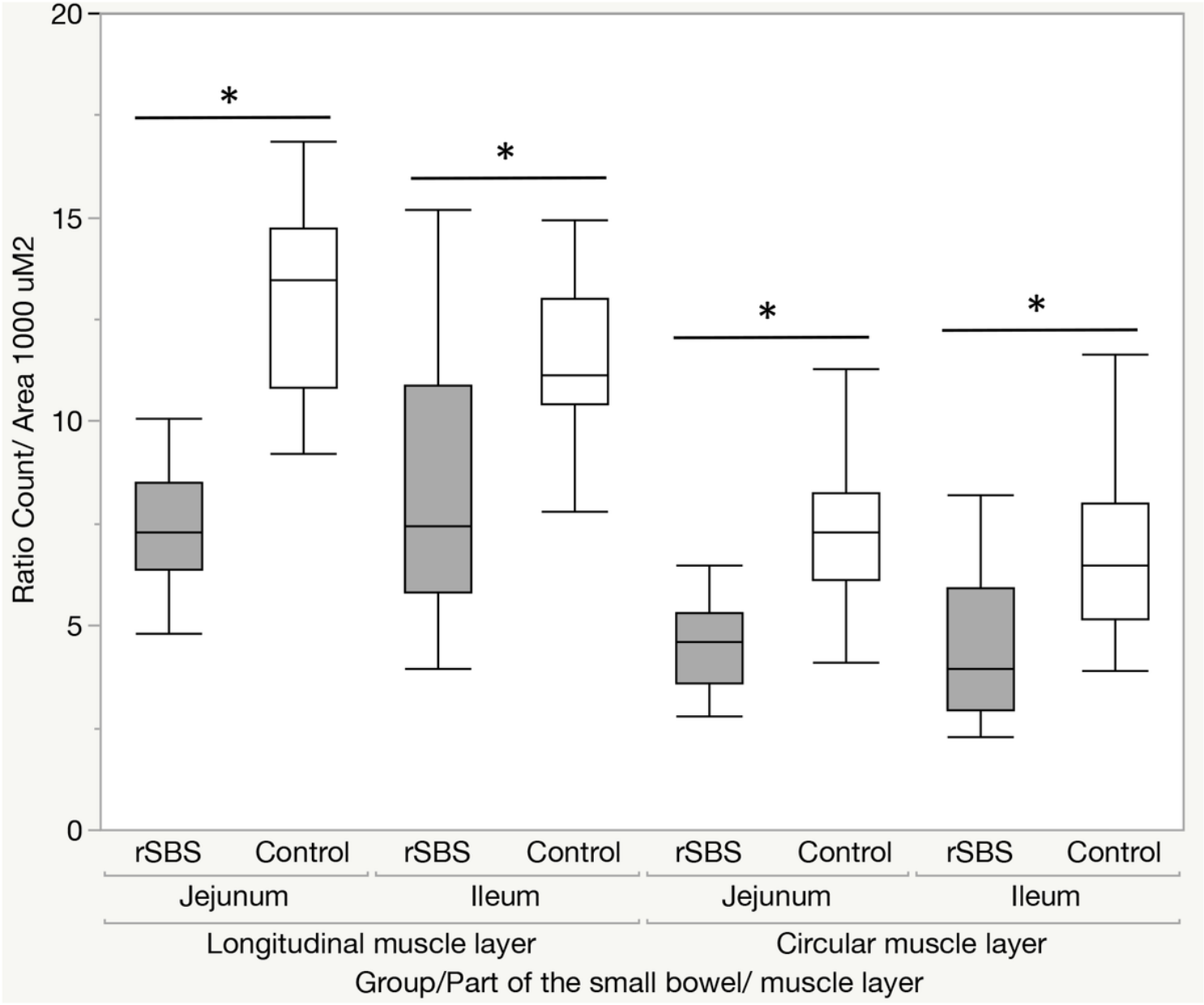

Figure 6

Number of nuclei in 1000 μm^2 of the area of muscle layer (rat). The comparison between control (Control) and short bowel syndrome (rSBS) revealed a significant increase number of nuclei in 1000 μm^2 of the area of muscle layer in rSBS compared to control in jejunum und ileum. Values: median, the top and bottom of the box represent the seventy-fifth and twenty-fifth percentile. The whiskers indicate the maximum and minimum (not including outliers). Wilcoxon test: * $p<0.0001$.

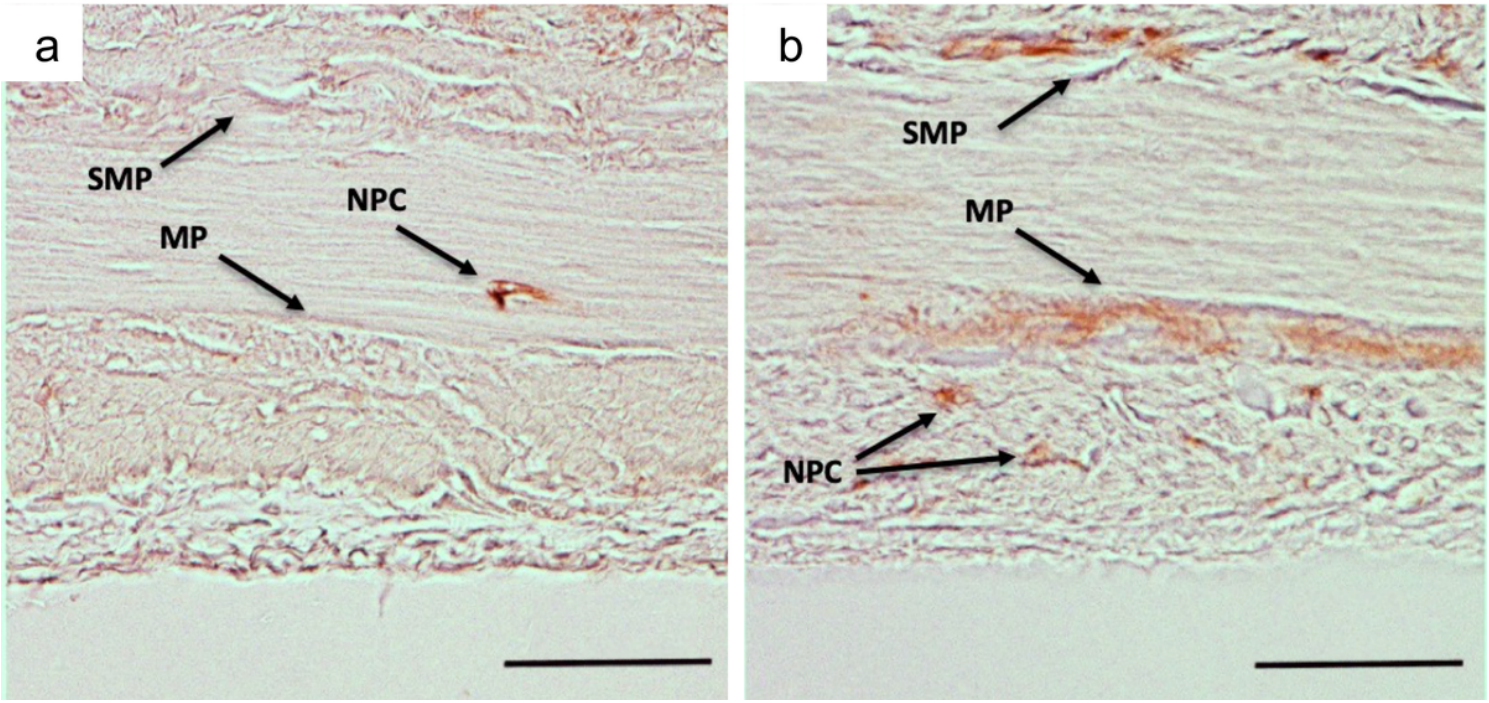

Figure 7

Nestin peroxidase stained ganglion of myenteric plexus a - control group, b - short bowel syndrome (rSBS) group (rat). Sections were stained two weeks after surgery. Arrows indicate: MP - plexus myentericus, SMP -plexus submucosus, NPC - nestin positive cells in muscle layer. In rSBS group myenteric plexus, plexus submucosa and some cells in muscle layer are nestin positive. Scale bar is 50 μm.

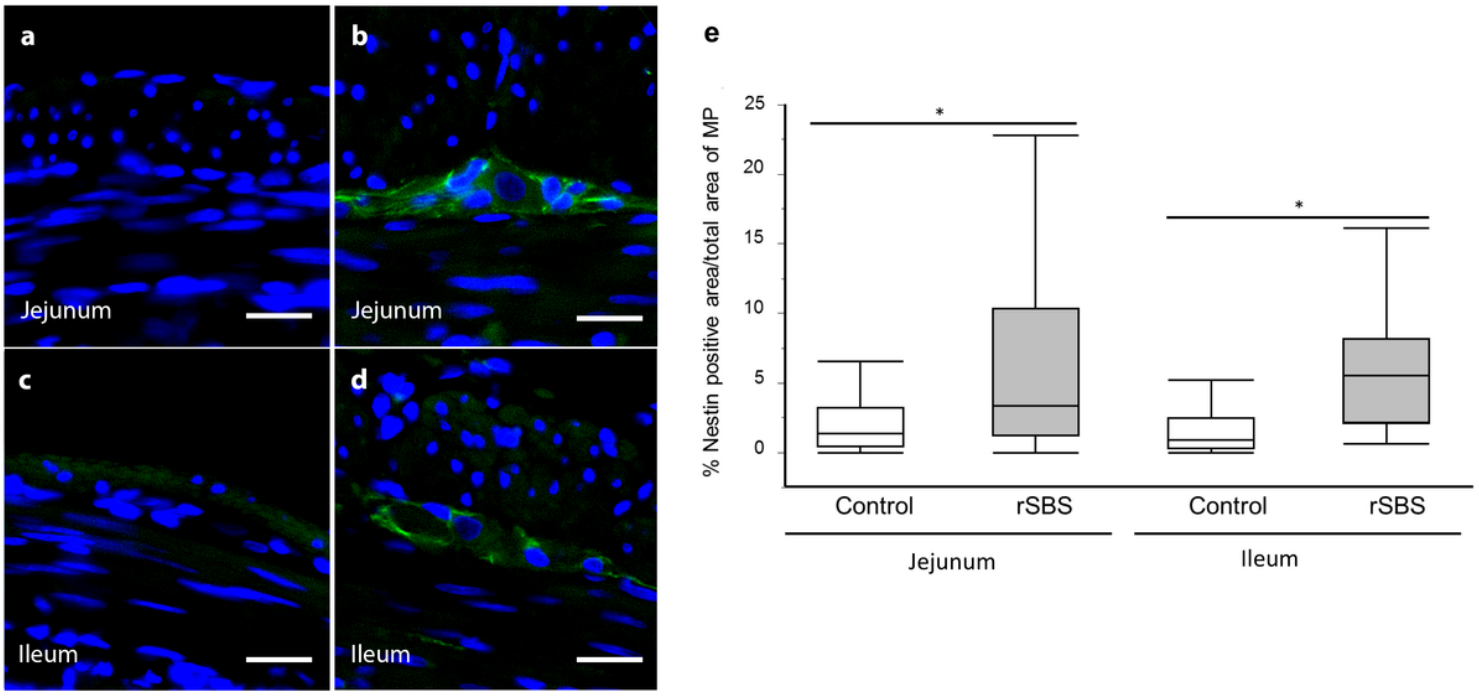

Figure 8

Nestin fluorescence stained ganglion of myenteric plexus of the small intestine. a and c- control group, b and d – short bowel syndrome (rSBS) group (rat). Nestin fluorescence – green colored, e - ratio of nestin positive areas within the myenteric plexus compared between (Control) and short bowel syndrome (rSBS). The rSBS small intestine presents more nestin positive areas within the myenteric plexus. Values: median, the top and bottom of the box represent the seventy-fifth and twenty-fifth percentile. The whiskers indicate the maximum and minimum (not including outliers). Wilcoxon test: * p<0.0001. Scale bar is 20 μm.

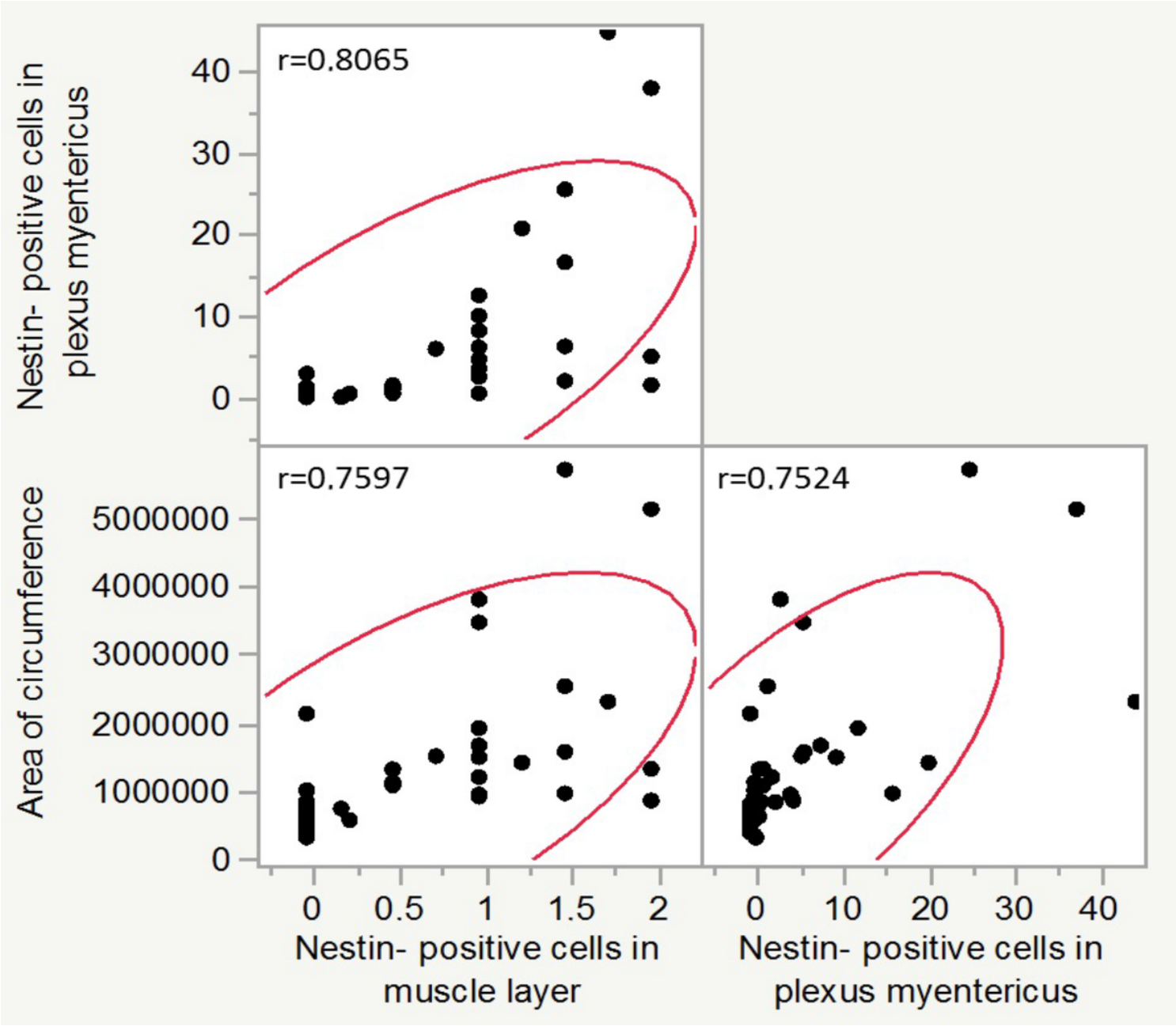

Figure 9

Spearmen's correlation between the area of muscle circumference and the upregulation of nestin expression in the myenteric plexus and in the muscle layer (rat).

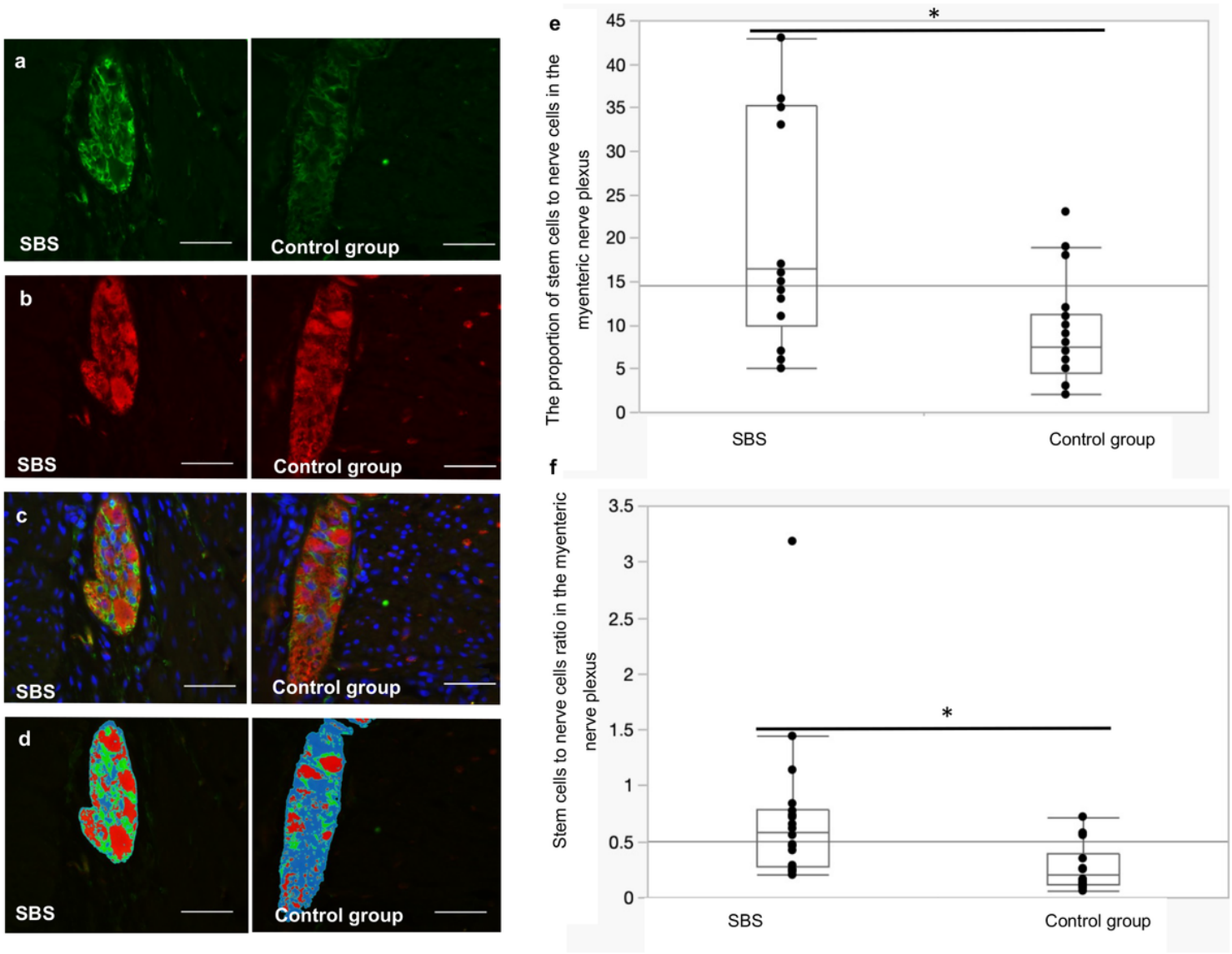

Figure 10

Ganglion of myenteric plexus (Plexus myentericus) in a biopsy specimen of the human small intestine. Immunofluorescence staining Stem cells: Nestin (green), neurons: PGP 9.5 (red), cell nuclei: DAPI (4',6-Diamidin-2-phenylindol, Dihydrochlorid) (blue). A: stem cell research, b: study of nerve cells, c: analysis of double staining (stem cells as well as nerve cells), d: mapping of the myenteric nerve plexus (green – stem cells, red – neurons), e – The proportion of the area of stem cells to the area of the nerve cells in a cross section of the myenteric nerve plexus, f – Stem cells to nerve cells ratio in the myenteric nerve plexus Values: median, the top and bottom of the box represent the seventy-fifth and twenty-fifth percentile. The whiskers indicate the maximum and minimum. Wilcoxon test: * $p<0.0001$. Scale bar is 50 µm.